Title

Engineering a Thermostable Keto Acid Decarboxylase Using Directed Evolution and Computationally Directed Protein Design

Journal

ACS Synthetic Biology, 6(4)

ISSN

2161-5063

Authors

Soh, Lemuel MJ
Mak, Wai Shun
Lin, Paul P
et al.

Publication Date

2017-04-21

DOI

10.1021/acssynbio.6b00240

Peer reviewed

ACS SyntheticBiology

Letter

pubs.acs.org/synthbio

Engineering a Thermostable Keto Acid Decarboxylase Using Directed Evolution and Computationally Directed Protein Design

Lemuel M. J. Soh,[†] Wai Shun Mak,[§] Paul P. Lin,[†] Luo Mi,[†] Frederic Y.-H. Chen,[†] Robert Damoiseaux,[∥,⊥] Justin B. Siegel,[§] and James C. Liao*[,†,‡,#]

[†]Department of Chemical and Biomolecular Engineering, and [∥]Department of Molecular and Medicinal Pharmacology, University of California, Los Angeles, 420 Westwood Plaza, Los Angeles, California 90095, United States

[‡]UCLA-DOE Institute of Genomics and Proteomics, 420 Westwood Plaza, Los Angeles, California 90095, United States

[§]Department of Chemistry, Biochemistry & Molecular Medicine, and the Genome Center, University of California Davis, One Shields Avenue, Davis, California 95616, United States

[⊥]California NanoSystems Institute, 420 Westwood Plaza, Los Angeles, California 90095, United States

[#]Academia Sinica, 128 Academia Road, Section 2, Nankang, Taipei 115, Taiwan, R.O.C

Supporting Information

ABSTRACT: Keto acid decarboxylase (Kdc) is a key enzyme in producing keto acid derived higher alcohols, like isobutanol. The most active Kdc's are found in mesophiles; the only reported Kdc activity in thermophiles is 2 orders of magnitude less active. Therefore, the thermostability of mesophilic Kdc limits isobutanol production temperature. Here, we report development of a thermostable 2-ketoisovalerate decarboxylase (Kivd) with 10.5-fold increased residual activity after 1h preincubation at 60 °C. Starting with mesophilic *Lactococcus lactis* Kivd, a library was generated using random mutagenesis and approximately 8,000 independent variants were screened. The top single-mutation variants were recombined. To further improve thermostability, 16 designs built using Rosetta Comparative Modeling were screened and the most active was recombined to form our best variant, LLM4. Compared to wild-type Kivd, a 13 °C increase in melting temperature and over 4-fold increase in half-life at 60 °C were observed. LLM4 will be useful for keto acid derived alcohol production in lignocellulosic thermophiles.

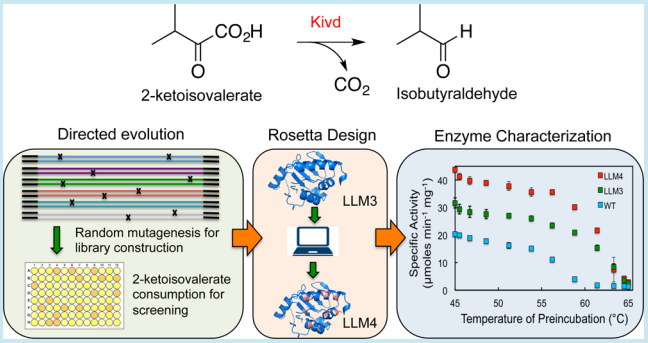

KEYWORDS: *thermostability, keto acid decarboxylase, high-throughput screening, protein design, directed evolution, isobutyl alcohol*

Keto acid decarboxylases (Kdc) are an important group of enzymes crucial to the production of keto acid derived alcohols,[1] including 1-propanol,[2] 1-butanol,[2] isobutyl alcohol,[3−7] 2-methyl-1-butanol[8] and 3-methyl-1-butanol.[9] Despite their importance, there are only two reported enzymes from thermophiles with Kdc activity, both of them homologues of the acetolactate synthase (Als) enzyme in different *Geobacillus* species.[3] Moreover, the activity of the only characterized, Gtng_0348 from *Geobacillus thermodenitrificans* is about 2 orders of magnitude lower than that of the most active Kdc from mesophile *Lactococcus lactis*, even after a heat treatment at 50 °C for both enzymes.[3] This *L. lactis* Kdc is a catabolic 2-ketoisovalerate decarboxylase (Kivd) whose main activity is to catalyze the decarboxylation of 2-ketoisovalerate to isobutyraldehyde, a crucial enzymatic step needed to divert flux from the valine biosynthesis pathway to isobutyl alcohol production. Kivd shares some structural similarity to pyruvate decarboxylase (Pdc), which also lacks a satisfactory thermostable homologue for heterologous expression at elevated temperatures.[10,11]

Kivd has been overexpressed to produce isobutyl alcohol in numerous microorganisms,[1,3−7] most recently at 50 °C in *Clostridium thermocellum*,[6] a lignocellulolytic thermophile of potential industrial importance. Production at an elevated temperature is desirable when using lignocellulosic feedstocks, as higher temperatures promote cellulose deconstruction.[12−16] Therefore, engineering a highly active and thermostable Kivd is a logical approach toward the further improvement of metabolically engineered isobutyl alcohol production in lignocellulolytic thermophiles.

To increase the thermostability of Kivd, a high-throughput screening process was developed as illustrated in Figure 1A. Briefly, we adapted a screening method based on absorbance changes at 315 nm that directly measured the consumption of 2-ketoisovalerate (KIV)[17] to high-throughput automation. The stability of KIV at elevated temperatures was confirmed to allow screening to occur at 50 °C, and proper controls were

Received: August 28, 2016
Published: January 4, 2017

DOI: 10.1021/acssynbio.6b00240
ACS Synth. Biol. 2017, 6, 610−618

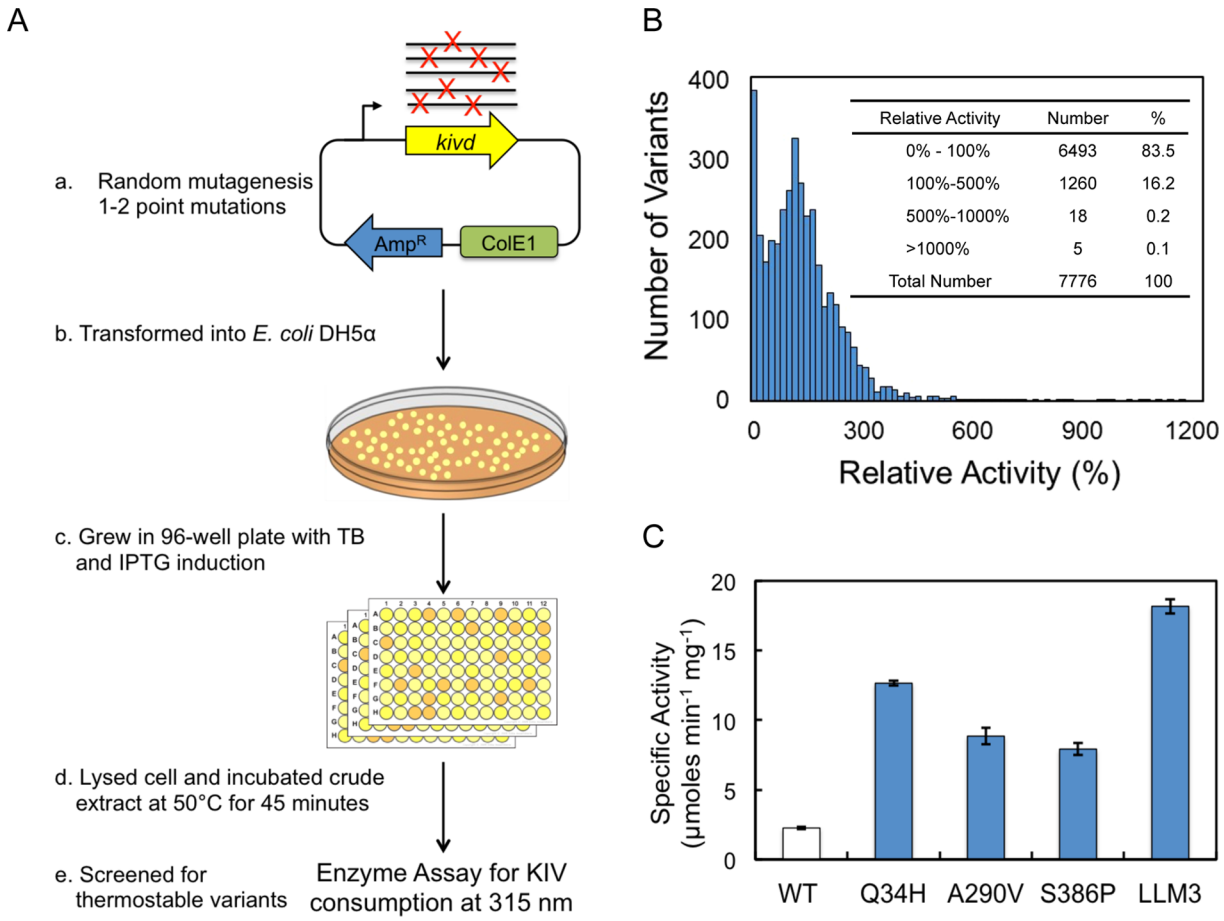

Figure 1. Identification of thermostable Kivd variants using high throughput screening: (A) summary of mutagenesis and screening; (B) distribution of relative crude extract activities compared to wild-type Kivd after 45 min heat treatment at 50 °C. (Variants with no measurable activity not plotted). (C) Specific activity of purified single mutation variants and LLM3, the recombination of all three single mutations, measured by NADH-coupled assay at 50 °C after 1 h of preincubation at 60 °C. The error bars represent the standard deviation of three independent repeats.

used to ensure that the change of absorbance is solely due to Kivd activity. For effective automation, the protocol was made simple and robust. To this end, a few criteria had to be fulfilled. First, an appropriate and convenient cell lysis method had to be determined that would ensure quality readout without interference from cell debris. Second, the reaction time of the enzyme assay had to be optimized to balance throughput and accuracy of enzyme activity measured. An end point enzyme assay was chosen instead of measuring a time course to further increase the throughput.

It is worth noting that during the development of a high throughput screen, the consistency of automated processing should be properly examined. For instance, one challenge observed during screen development was the significant amount of cell debris and precipitate formed after lysis and heat treatment at 50 °C. Despite the availability of more laborious methods such as centrifugation to pellet the debris, it was found that simply allowing the debris to settle and setting the liquid handler to draw from the top at the slowest speed could consistently ensure that no debris is transferred to the final assay solution. The simplicity of the screen is also of practical importance. For example, even though there are other ways to incubate the cell lysate that could be more precise, air incubation was found to be most convenient, and the results were without adverse effects from potential heat transfer limitations.

A random mutagenesis library of Kivd was made using error-prone PCR with only 1 to 2 point substitutions introduced per *kivd* gene. Such a low mutation rate was chosen because most mutations are deleterious and multiple mutations often completely inactivate the enzyme.[18] In so doing, the percentage of active enzymes within our library is maximized.

Independent transformants were picked into 96-well plates, induced for protein expression, and subsequently lysed by detergent. The crude cell extract was heat challenged at 50 °C for 45 min before starting the enzyme assay. The screening temperature of 50 °C and incubation time were tested iteratively to ensure that the wild-type Kivd enzyme (positive control) had activity that could be detected by our screen consistently. The change in KIV characteristic UV absorbance before and after the enzyme assay, normalized to initial cell density, was used as an indicator for Kivd activity retained after heat treatment.

Following the aforementioned screening protocol, approximately 2000 variants were picked and screened in each round, with a total of 4 rounds. The activity of these variants, as a percentage of the wild type, is plotted in Figure 1B. Two peaks were clearly evident in the histogram. First, there were a large number of variants (about 50%) that did not have any measurable activity, either due to failure to fold or complete loss of thermal stability at 50 °C. Second, many of the variants had activity clustered around the wild type. This cluster most

DOI: 10.1021/acssynbio.6b00240
ACS Synth. Biol. 2017, 6, 610−618

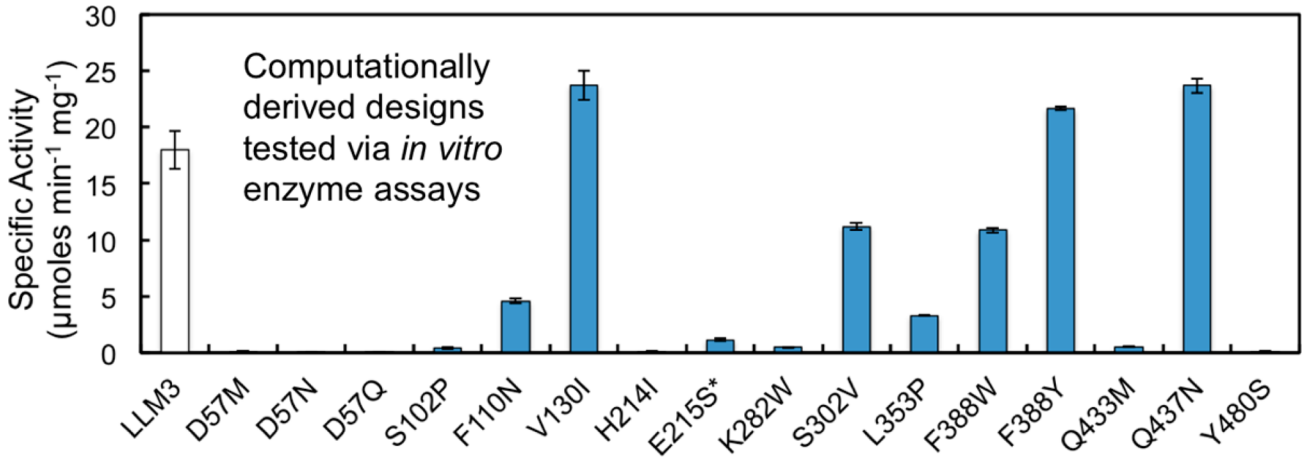

Figure 2. Sixteen mutations derived using Rosetta design were recombined individually with LLM3, and the enzymes were purified. Specific activity was measured by NADH-coupled assay at 50 °C after 1 h preincubation at 60 °C. V130I, F388Y, and Q437N were found to have increased activity over LLM3. *E215S had an added mutation I305P as part of the computational design. LLM3_V130I has the highest activity after preincubation at 60 °C for 1 h and is renamed LLM4.

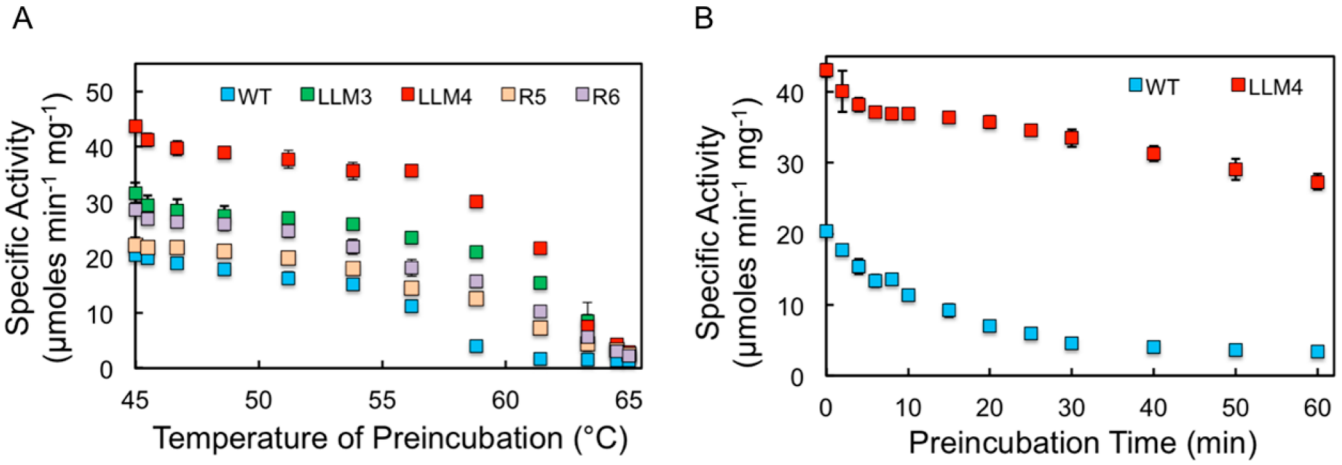

Figure 3. Characterization of purified thermostable Kivd variants. (A) Plot of Kivd specific activity after 1 h preincubation at various temperatures. LLM4, best variant after recombining V130I (computationally derived) with LLM3; LLM3, best variant after recombination of Q34H, A290V, and S386P mutations (directed evolution); R6, mutations V130I, Q437N, and F388Y were recombined with LLM3 to form a 6-mutation Kivd variant; R5, mutations V130I and Q437N were recombined with LLM3 to form a 5-mutation Kivd variant; WT, wild-type Kivd. (B) Plot of Kivd LLM4 and WT specific activity at 60 °C heat preincubation for various times. Specific activities measured by NADH consumption at 50 °C. The error bars represent the standard deviation of three independent repeats.

likely consists of Kivd variants that have similar thermal stability as the wild type but some difference in activity. With almost 8000 independent variants screened, about 70% of the single substitutions possible in Kivd would likely have been covered. The screening results mostly corroborate earlier protein evolution studies that show the vast majority of single amino acid mutations are deleterious or at best neutral, with only 0.01 to 1% being beneficial.[18−22]

From that library of about 8000 independent transformants, 12 of the most active variants were selected and sequenced. Some of the variants had mutations that did not code for amino acid changes, and their increased activity is likely due to an increase in expression of Kivd in *E. coli*. These were discarded as the thermostable Kivd variant would eventually be used in other thermophiles such as *C. thermocellum*. From the 12 mutants sequenced, 3 single point substitutions (Q34H, A290V, and S386P) were identified as possibly increasing thermostability. A290V appeared multiple times with the same codon change in independent variants through different rounds of mutagenesis and screening.

Those single-mutation Kivd variants were purified and characterized. Although it is simple to directly measure the consumption of KIV at 315 nm, this assay is not ideal for further detailed characterization due to its low sensitivity (extinction coefficient of KIV is 26.8 M^{-1} cm^{-1} at 315 nm). Therefore, a NADH-coupled enzyme assay[3] which is much more sensitive (extinction coefficient of NADH is 6220 M^{-1} cm^{-1} at 340 nm) was chosen for all characterization work of the purified Kivd variants. A 60 °C 1 h heat preincubation was performed in the thermocycler, and activity was measured at 50 °C using the NADH-coupled enzyme assay. The thermal stability effect of all three mutations was confirmed. Compared to the wild type, Q34H had a 5.5-fold increase, A290V had a 4-fold increase, and S386P had a 3.5-fold increase in specific activity after a 1 h preincubation at 60 °C (Figure 1C).

Since the effects of thermostable mutations are likely additive,[23] these three stabilizing mutations were recombined.

DOI: 10.1021/acssynbio.6b00240
ACS Synth. Biol. 2017, 6, 610−618

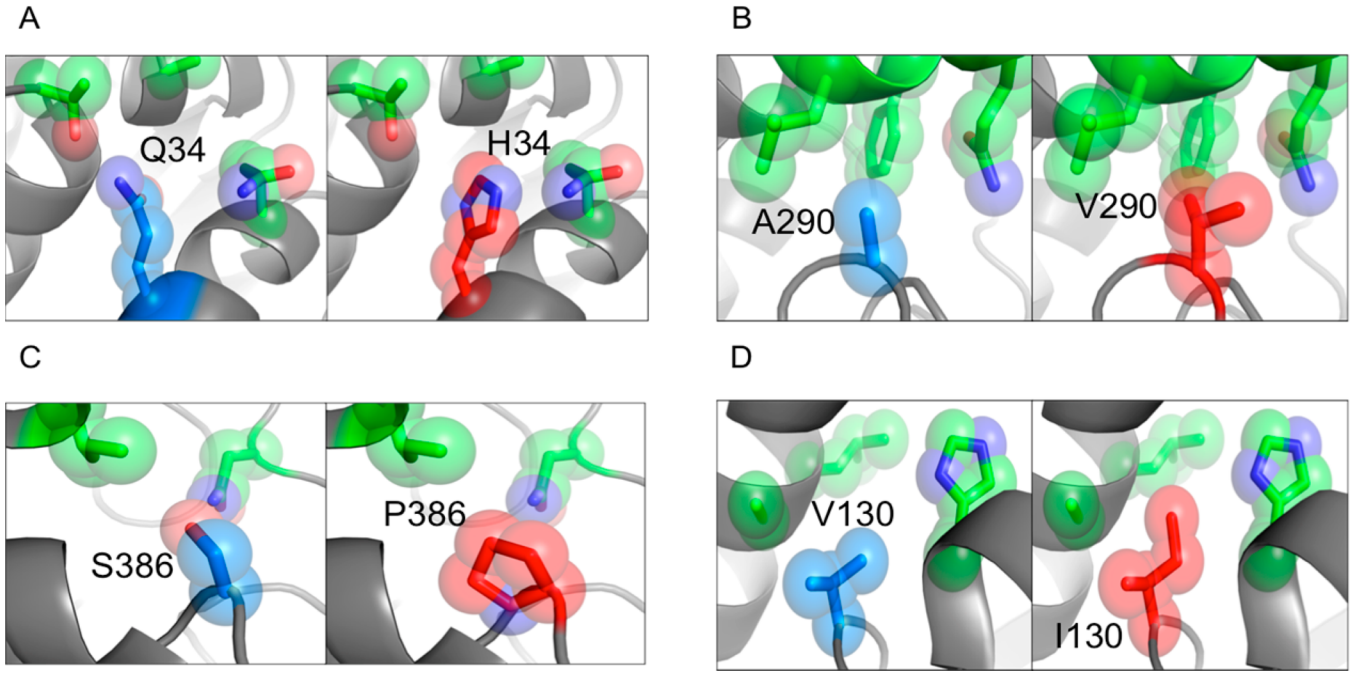

Figure 4. Local environments of beneficial Kivd mutations (A) Q34H, (B) A290V, (C) S386P, and (D) V130I with the native and mutated residue depicted in blue and red, respectively. Mutations Q34H, A290V, and S386P were identified through directed evolution and mutation; V130I was identified *via* computationally directed protein design. The mutations A290V and V130I are predicted to improve hydrophobic packing of the local environment.

The recombined *kivd* variant was named LLM3. The specific activity of LLM3 at 60 °C is 8-fold higher than that of the wild type (Figure 1C). The T_{50} of LLM3, which is the temperature at which the enzyme loses half of its maximum activity after an hour incubation, was measured to be 60.3 °C (Figure 3A). This represents an increase over the wild-type T_{50} of 56.1 °C by 4.2 °C (Figure 3A). The T_{50} of wild-type Kivd measured in this study is similar to that previously reported.[3] This result indicates that LLM3 has substantial activity at the elevated temperature of 60 °C.

In addition to high-throughput screening of Kivd mutant libraries, computationally directed protein design of thermostabilizing mutations was performed using Foldit,[24] a graphical-user-interface to the Rosetta Molecular Modeling Suite. Mutations that improved packing or introduced new hydrogen bonds outside of the enzyme active site were explored based on previous observations that such mutations can significantly increase thermostability.[25] Sixteen mutants were designed using this approach and experimentally characterized after recombination with LLM3 (Figure 2).

While the majority of the mutations significantly decrease enzyme activity, mutations V130I, Q437N, and F388Y increase the activity of LLM3 at 60 °C by 32%, 31%, and 20%, respectively (Figure 2). The mutation V130I is predicted to improve core hydrophobic packing with the additional methyl group on isoleucine. The Q437N mutation lies at the Kivd homodimeric interface, and its amide carbon is predicted to be 4.5 Å from the same carbon atom on its dimeric partner. These two partnering Q437N residues are predicted to stabilize the interface by forming a hydrogen bond between their carbonyl oxygen and amide nitrogen. The mutation F388Y introduces a hydroxyl group, which is predicted to satisfy a previously unsatisfied hydrogen bond on the carbonyl oxygen of the L254 backbone. Mutations V130I and Q437N were recombined with LLM3 to form a 5-mutation Kivd variant named R5. Mutations V130I, Q437N, and F388Y were recombined with LLM3 to form a 6-mutation Kivd variant named R6. Kinetic characterization of variant R5 and R6 shows that the effects of these mutations are not additive. They exhibit similar or lower activity and thermostability compared to LLM3 (Figure 3A). The origin of these nonadditive effects is unclear as each of these three mutations are 15−30 Å apart from each other. The variant LLM3_V130I (renamed LLM4) has the highest thermostability of all the mutants tested, with its T_{50} being 4.3 °C higher than native Kivd.

Even though the T_{50} of LLM4 did not change significantly from that of LLM3, the large increase in specific activity of LLM4 at 60 °C is a functional advantage for metabolic engineering (Figures 2 and 3A). The half-life of LLM4 measured at 60 °C was more than 1 h, which is more than a 4-fold increase over the wild type's half-life of 14.0 min (Figure 3B). The specific activity of LLM4 at 60 °C is 10.5-fold higher than that of the wild type.

To determine the potential mechanisms by which the mutations identified *via* directed evolution (Q34H, A290 V and S386P) conferred thermostability, a model of the Kivd protein was acquired *via* homology modeling[26] by using the crystal structure of *L. lactis* branched-chain keto acid decarboxylase[27] (PDB ID: 2VBF) which shares an 88% sequence identity with the wild-type Kivd. The acquired Kivd model was visualized and further studied using Pymol software (Figure 4).[28] The three amino acid mutations (Q34H, A290V, and S386P) identified *via* directed evolution are all located near the protein surface and far away from enzyme active site.

Besides homology modeling, circular dichroism spectroscopy (CD) of both wild-type Kivd and LLM4 were measured to further analyze the combined structural effects of various point mutations (Figure 5). CD spectra results indicate that wild-type Kivd and LLM4 possess similar structures at 25 °C, which is consistent with the fact that both WT and LLM4 are active at

DOI: 10.1021/acssynbio.6b00240
ACS Synth. Biol. 2017, 6, 610−618

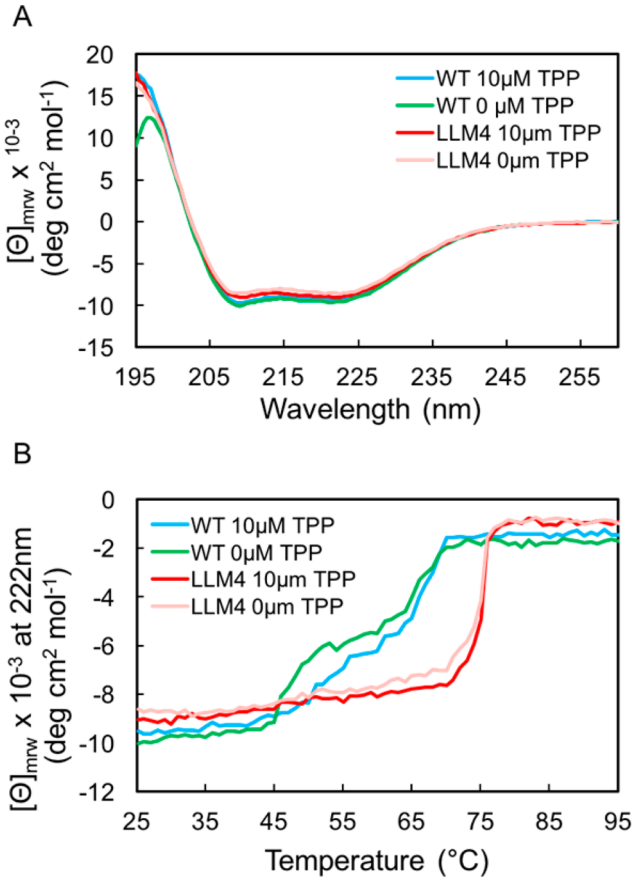

Figure 5. Structure and thermal stability analysis of Kivd WT and LLM4 with and without TPP: (A) CD spectra at 25 °C of WT and LLM4; (B) thermal unfolding profiles of WT and LLM4 monitored by change of mean residual ellipticity as a function of temperature at 222 nm.

physiological conditions (Figure S4). Furthermore, results are similar to or without thiamine pyrophosphate (TPP), a crucial cofactor for the enzyme,[29] for both WT and LLM4 variant.

Moreover, monitoring ellipticity changes while heating proteins enables the determination of the unfolding temperature T_m, defined as the temperature at which 50% of the protein is denatured. The wild-type Kivd without TPP was found to have a lower T_m of 55.8 °C compared to the T_m of wild type with TPP at 61.3 °C. This suggests that wild-type Kivd without TPP is structurally more unstable, which is consistent with the fact that TPP is responsible for proper assembly of the active tetramer in the Pdc family.[29−31] In comparison, the T_m values of LLM4 were both higher at 73.8 and 74.6 °C, without and with TPP, respectively. Thus, LLM4 had a significant 13.3 °C improvement in T_m when TPP is included in the buffer (Figure 5). Intriguingly, the absence of TPP did not negatively affect the T_m of LLM4 by much, suggesting that the Kivd variant may have stabilized the overall structure of the enzyme so that the active site function would not be affected adversely at higher temperature. Noticeably, all T_m were higher than T_{50} by around 5 to 15 °C, which is typical as enzymes normally first lose their function before degrading.[32]

Further characterization was also carried out on LLM4 to determine its suitability for other functions. First, kinetic parameters at 50 °C were characterized for LLM4 and wild-type Kivd. Compared to the wild type, LLM4 had a similar K_m and a k_{cat} 2-fold greater (Table 1). The k_{cat}/K_m value of LLM4 is 24.38, compared to the 11.15 value of the wild-type enzyme

Table 1. Kinetic Parameters of the Wild Type and Mutant 2-Ketoisovalerate Decarboxylase Measured at 50°C

Kivd variant	K_m (mM)	k_{cat} (s^{-1})	k_{cat}/K_m (mM^{-1} s^{-1})
LLM4	1.55 ± 0.03	37.89 ± 0.22	24.38
WT	1.60 ± 0.03	17.90 ± 0.28	11.15

(Table 1). Thus, LLM4 has similar affinity but a much higher turnover rate than the wild-type Kivd. Furthermore, it is observed that LLM4 has a higher specific activity after heat incubation at temperatures ranging from 45 to 65 °C (Figure 3A). LLM4 specific activities on other substrates similar to 2-ketoisovalerate in structure were also measured in this study. LLM4 had an observably higher specific activity for all the substrates, especially pyruvate, when measured at 50 °C (Figure 6). Thus, LLM4 is thermostable at 60 °C while improving catalytic activity on 2-ketoisovalerate or other substrates.

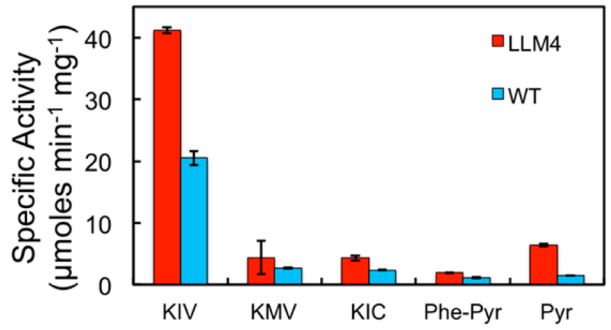

Figure 6. Specific activity of purified LLM4 to different keto acid substrates. KIV, 2-ketoisovalerate; KMV, 2-keto-3-methyl-valerate; KIC, 2-keto-4-methyl-pentano-ate; Phe-Pyr, phenylpyruvate; Pyr, pyruvate. Specific activities measured by NADH consumption at 50 °C. The error bars represent the standard deviation of three independent repeats.

Despite screening at 50 °C for more active variants, we found variants that were substantially more thermostable than the wild type at 60 °C. In fact, a higher specific activity than the wild type was observed at all tested temperatures higher than 45 °C. Besides being useful for isobutyl alcohol production in thermophiles such as *C. thermocellum*, it is expected that Kivd LLM4 could be useful for the production of higher alcohols in a variety of organisms[1,4,5] and also in cell-free systems.[33] The absorbance-based screen used for high throughput evolution is not only simple but can also be modified for the directed evolution of other keto-acid decarboxylases.

METHODS

Bacterial Strains and Plasmid Construction. All plasmid construction and enzyme expression was done using *E. coli* NEB 5-alpha strain (New England Biolabs, Ipswich, MA). All plasmids were constructed by DNA assembly techniques.[34] Oligonucleotides were purchased from IDT technologies (San Diego, CA). Both vector and inserts (target genes) were amplified by PCR using KOD Hot Start DNA polymerase (EMD Millipore, Billerica, MA). The PCR template was digested by DpnI digestion at 37 °C for 1 h (New England Biolabs). PCR products were purified by DNA clean and

DOI: 10.1021/acssynbio.6b00240
ACS Synth. Biol. 2017, 6, 610−618

concentrator kit (Zymo Research, Irvine, CA). The vector and insert were mixed with Gibson Assembly Master Mix (New England Biolabs) and incubated at 50 °C for 1 h. The assembly product was then transformed to the *E. coli* strain mentioned above. Plasmids meant for Kivd library generation were extracted by miniprep (Qiagen, Hilden, Germany) and sent for DNA sequencing (Laragen, Culver City, CA). *kivd* (*L. lactis*) was amplified from the pSA65 plasmid[35] and a modified pQE9 vector was used to construct plasmid pLS02. All solid and liquid media used for growing strains with pLS02 were supplemented with 200 μg/mL of carbenicillin.

Library Construction. Error-prone PCR was performed on *kivd* using GeneMorph II random mutagenesis kit (Agilent Technologies, San Jose, CA). To achieve 1 to 2 mutations per *kivd* gene, 300 ng of the template gene was used with 25 cycles of PCR. The *kivd* random mutagenesis library was used to construct plasmid pLS02 as described above for the wild-type gene. Transformants were plated on Bioassay Q-trays (Molecular Devices, Sunnyvale, CA) with LB agar. Twelve independent transformants were randomly picked and sequenced to ensure that the desired mutation rate was achieved.

Cell Lysis for High Throughput Screening. Cells were grown up to an OD_{600} of 0.6 to 0.8 in 96-well plates before being lysed. This OD_{600} is recorded for normalization of the assay results. Despite the efficacy of beads and sonication, they were laborious to use in high throughput screening. Commerical detergent Bugbuster (no. 70921, EMD Millipore) was found to be simple and effective for screening the library. Instead of removing cell debris by centrifugation and resuspension, the process was simplified by adding 80 μL of Bugbuster of 3× Bugbuster reagent to a 150 μL cell culture and incubating for 20 min at room temperature. The cell lysate was then used in the crude extract enzyme assay described in the following section. The 3× Bugbuster reagent is made by diluting Bugbuster 10× Protein Extraction Reagent (no. 70921, EMD Millipore) to a 3× concentration with an appropriate amount of Milli-Q water.

KIV Absorbance-Based Kivd Assay. A simple Kivd assay[17] was adapted for use in high throughput screening with crude extract cell lysates. Substrate 2-ketoisovalerate had an absorbance peak at 315 nm after a spectral scan on a DU-800 spectrophotometer (Beckman Coulter, Brea, CA) and substrate disappearance at that wavelength was used as the basis of the screen. The other components, namely magnesium chloride, thiaminpyrophosphate (TPP), and sodium phosphate buffer required in our crude extract enzyme assay were also checked for overlapping absorbance. Only TPP had substantial absorbance in the UV range but this readout was stable at the assay conditions and thus was not a concern. A possibility for signal interference was further reduced by using a lens during screening that aliased lower wavelength UV.

The cell lysate obtained as described in the section Cell Lysis for High Throughput Screening was subject to a 45 min air incubation at 50 °C. The cell debris and precipitate were allowed to settle and only 30 μL of supernatant was transferred to a fresh UV-transparent plate (no. 655801, Greiner, Monroe, NC). A 170 μL sample of enzyme master mix was added to make a final concentration of 5 mM $MgCl_2$, 1.5 mM TPP, and 60 mM 2-ketoisovalerate in 50 mM pH 6.5 sodium phosphate buffer. OD_{315} is measured before air incubating at 50 °C for 2 h. After 2 h, OD_{315} is measured again to obtain the end-point enzyme assay reading. The enzyme thermostability score of each independent transformant is calculated by (beginning OD_{315} − ending OD_{315})/OD_{595}. The final results were normalized by OD_{595} of the corresponding cell cultures to minimize the effect of different protein amounts.

High Throughput Screening. All screening was performed in the Molecular Screening Shared Resource, UCLA. All optical density (OD) measurements were performed on a Victor 3 V plate reader (PerkinElmer, Waltham, MA); 96-well plates (#3370, Corning, Corning, NY) were filled with 150 μL of terrific broth (TB) medium supplemented with 3% (v/v) glycerol. Single colonies were picked into plates using Genetix Qbot colony picker (Molecular Devices, Sunnyvale, CA). The plates were incubated at 37 °C for 5 h. Following this, a copy of all the picked colonies were made into 96-well low-profile plates (X6023, Molecular Devices) containing TB medium supplemented with 10% glycerol (v/v) on Genetix Qbot. This storage copy was grown overnight at 37 °C, covered with aluminum sealing film (no. 6569, Corning) and stored at −80 °C. After the copies were made, 10 μL of 16 mM IPTG was added to make a final concentration of 1 mM for protein induction in the initial plates of the picked colonies. Protein induction continued for 12 h at 37 °C. After this time, an automated ORCA arm (Beckman Coulter, Brea, CA) moved the plates between different stations for screening. The screen was scheduled and controlled using the Sami automation platform (Beckman Coulter, Brea, CA). Plates were transferred from the incubator to BioMek FX (Beckman Coulter, Brea, CA) and shaken for 1 min at 1000 rpm before OD_{595} was measured. Cells were lysed by adding 80 μL Bugbuster of 3× Bugbuster reagent. For 20 min, the cells are lysed at room temperature and cell debris collects to the bottom of the well. A BioMek FX with 200 μL of AP 96 pipetting head (Beckman Coulter, Brea, CA) is used to transfer 30 μL of cell lysate to fresh UV-transparent 96-well plates (no. 655801, Greiner, Monroe, NC). 170 μL of enzyme master mix was added, and the crude extract Kivd enzyme assay is conducted as described above in the section KIV Absorbance-Based Kivd Assay.

Computational Simulations. The 3D model of Kivd used for rational design was built using the Rosetta Comparative Modeling protocol.[36] Fragments sets[37] and three-dimensional evolutionary constraints[38] were generated using crystal structure PDB 2VBG. A total of 1000 models were generated, and the model with the lowest energy was used as the homology model of Kivd. Foldit was used to evaluate the effects of mutations on thermostability. The changes in rosetta energy of the mutated residue and the protein pose after repacking were used to select candidate mutations for experimental characterization.

Protein Purification. The highest activity variants obtained from the high throughput screen were selected and sequenced. Kivd variants that resulted in an amino acid substitution were purified. The plasmid construct pLS02 used for screening attaches a His-tag to the 5′ end of Kivd for enzyme purification. Wild-type Kivd and variants were purified as follows: NEB-5alpha cells containing the pLS02 plasmid from screening were used. The respective cell lines were cultured in 200 mL of LB medium. After the cells reached mid-log phase, IPTG was added to a final concentration of 1 mM to induce protein expression followed by incubation at room temperature with shaking on the Excella E5 platform shaker (New Brunswick Scientific) at 250 rpm overnight. The cells were pelleted by centrifugation for 30 min at 6000*g* at 4 °C. Recombinant proteins were purified using the Profinia protein purification

DOI: 10.1021/acssynbio.6b00240
ACS Synth. Biol. 2017, 6, 610−618

instrument (Bio-Rad, Hercules, CA) according to the manufacturer's protocol. The Bio-Rad native IMAC protocol was selected at standard flow rate and standard wash time and used in conjunction with the Profinia IMAC purification kit (no. 6200225, Bio-Rad). The buffer of the purified enzyme was changed to a 50% (w/v) ethylene glycol solution (no. 29810, Life Technologies, Carlsbad, CA) with 5 mM $MgCl_2$, 1.5 mM TPP and adjusted to pH6.5. Buffer was changed by centrifugation at 4 °C using an Amicon ultra 15 mL centrifugal filter (EMD Millipore) according to manufacturer's protocol. Protein concentration was measured using the quick start Bradford protein assay kit (Bio-Rad). The purified proteins were analyzed on 15% Mini-PROTEAN TGX stain-free gel (Bio-Rad) and visualized on the Bio-Rad Gel Doc EZ imager to ensure that the purity of Kivd variants are similar. Purified protein was stored at −20 °C and used for characterization as needed according to the protocol described in other sections. Multiple protein purifications were used for each of the experiments to characterize the Kivd variants.

Heat Incubation. Purified Kivd was preincubated at respective temperatures for duration as needed by the characterization test in a thermocycler (Mastercycler nexus GSX1 flexlid, Eppendorf, Hauppauge, NY). A 60 μL aliquot of the purified Kivd variant or wild type suspended in 50 mM pH 6.5 sodium phosphate buffer containing 5 mM $MgCl_2$ and 1.5 mM TPP was preincubated in each PCR tube.

NADH-Coupled Kivd Enzyme Assay. To characterize the purified Kivd variants, a more sensitive NADH-coupled enzyme assay was adapted from previous work.[3] The assay was conducted in 200 μL reaction mixtures in a UV-transparent 96-well plate (no. 3635, Corning). A 10 μL aliquot of purified Kivd variant was added to 190 μL of a fresh master mix solution to start the reaction. Similar to that in a previous report,[29] final concentrations of the reaction mixture were 5 mM $MgCl_2$, 1.5 mM TPP, 30 mM 2-ketoisovalerate, 140U of commercial alcohol dehydrogenase (A3263, Sigma-Aldrich, St. Louis, MO) and 0.2 mM NADH in 50 mM pH 6.5 sodium phosphate buffer. TPP is prepared fresh at the point of enzyme assays. The master mix was incubated at 50 °C for 5 min while the purified Kivd variant was incubated at room temperature for 5 min before the reaction was started. Reaction mixtures are shaken for 1 min at medium intensity on a PowerWave XS microplate spectrophotometer (Bio-Tek, Winooski, VT) while being incubated at 50 °C. The consumption of NADH is then measured at 340 nm absorbance on the PowerWave XS microplate spectrophotometer at 50 °C (Bio-Tek). Enzyme activity is calculated by using NADH extinction coefficient at 6220 M^{-1} cm^{-1} and a light path of 0.5533 cm. Specific activity is obtained through normalization of the activity by enzyme concentration.

Recombination. Recombination was performed after the increased thermostability of the Q34H, A290V, S386P, and V130I mutations were confirmed. Starting with the A290V variant, the other mutations were added with the appropriate primer design sequentially. Primers with a point substitution encoding for the appropriate additional mutation were used to amplify Kivd from the variant in a PCR. The resulting PCR products were assembled as described above in plasmid construction to reconstruct the plasmid pLS02. This pLS02 construct contained Kivd variant LLM4, with mutations Q34H, A290V, S386P, and V130I.

T_{50} determination. For the determination of T_{50}, the purified wild-type Kivd and variants were preincubated at temperatures ranging from 45 to 65 °C for 1 h using the temperature gradient function on the thermocycler (Mastercycler nexus GSX1 flexlid, Eppendorf, Hauppauge, NY). Following this, the NADH-coupled assay as described before was started by adding 10 μL of the preincubated purified enzyme to 190 μL of the enzyme master mix. Three independent repeats were conducted and the mean specific activities with standard deviation are plotted in Figure 3A. T_{50} values are computed as follows: First, a second order polynomial is fitted to the mean values plotted in Figure 3A using the MATLAB "fit" function. Next, to calculate the T_{50} for 1 h preincubation, the polynomial fit equation from Figure 3A was solved for the temperature at which half the original activity of Kivd would be lost using the appropriate MATLAB code.

Half-Life Determination. For the determination of half-life, multiple separate PCR tubes of the purified Kivd variant and wild type were preincubated at 60 °C. Time points from 0 to 60 min were determined and as the respective time point was reached, the appropriate PCR tube was removed from the thermocycler and stored at 4 °C until the purified Kivd enzyme assay (NADH-coupled assay) described before was started. The assay was started within an hour of the first sample being taken out from the thermocycler, and all samples were processed simultaneously. Three independent repeats were conducted and the mean specific activities with standard deviation were plotted in Figure 3B. Half-life values are computed as follows: First, a second order polynomial is fitted to the mean values plotted in Figure 3B using the MATLAB "fit" function. Next, to calculate the half-life at 60 °C, the polynomial fit equation from Figure 3B was solved for the preincubation time at which half the original activity of Kivd would be lost using the appropriate MATLAB code.

CD Spectroscopy. Before CD spectroscopy measurements, buffer of the purified protein was exchanged to 50 mM pH 6.5 sodium phosphate buffer with 5 mM $MgCl_2$ *via* dialysis (MWCO 3500, Spectrumlabs, CA) to ensure total elimination of TPP, imidazole, and glycerol in the solution as these compounds would affect absorption readouts. Samples were then prepared to the appropriate concentration (4.14 μM), with and without 10 μM of fresh TPP, which is around 2.5 mol equiv of the purified protein. CD spectrum was obtained by a JASCO J-815(JASCO, Japan) using 1 mm path length Suprasil quartz cells (Hellma, UK). Full wavelength data were collected at 25 °C, with the wavelengths ranging from 195 to 260 nm at 0.5 nm intervals. A protein unfolding curve was collected with a 1 °C interval at 222 nm after 5 min of incubation at each specific temperature. T_m was computed as follows. First, the acquired data were fitted by a sigmoid curve. Next, the first order derivative of the sigmoid curve was taken. The T_m was then determined by locating the local maxima of the derivative plot.

Kinetic Parameters and Substrate Specificity Determination. Kinetic parameter characterization was performed using the NADH-coupled enzyme assay with 2-ketoisovalerate concentrations varying from 0 to 10 mM. Three independent repeats were conducted. A second order polynomial fit was fitted to the mean values computed using the MATLAB "fit" function. Next, to calculate the K_m, the polynomial fit equation was solved using the appropriate MATLAB code for the 2-ketoisovalerate concentration at which half the maximum specific activity of Kivd (V_{max}) would be observed. k_{cat} numbers were calculated assuming the theoretical weight of a single Kivd subunit to be 61 kDa (Kivd is a homodimer). To test the

DOI: 10.1021/acssynbio.6b00240
ACS Synth. Biol. 2017, 6, 610−618

specific activity on different substrates, the NADH-coupled enzyme assay was conducted as described before, substituting 30 mM 2-ketoisovalerate with 30 mM of the appropriate substrate. Three independent repeats were conducted, and the mean specific activities with standard deviation were plotted in Figure 6.

■ ASSOCIATED CONTENT

Supporting Information

The Supporting Information is available free of charge on the ACS Publications website at DOI: 10.1021/acssynbio.6b00240.

The activity profile of Kivd variants LLM3_F388Y and LLM3_Q437N after preincubation at various temperatures for 1 h (Figure S1). The activity profile of all rational designs individually recombined with LLM3 after preincubation at various temperatures for 1 h (Figure S2). Comparison of two different buffers on Kivd enzyme activity (Figure S3). Specific activities of wild-type KIVD and LLM4 to 2-ketoisovalerate, at physiological temperatures of 22, 30, and 37 °C (Figure S4). SDS-PAGE of wild-type Kivd and variants (Figure S5). Distance between carbanion of TPP ylide and C-alpha of mutated amino acid residue in the proposed Kivd structure model (Table S1). Codon changes that did not code for amino acid substitutions (Table S2) (PDF)

■ AUTHOR INFORMATION

Corresponding Author

*E-mail: liaoj@g.ucla.edu.

ORCID

James C. Liao: 0000-0002-4580-7276

Notes

The authors declare no competing financial interest.

■ ACKNOWLEDGMENTS

This research was supported by the DOE BioEnergy Science Center (BESC). This material is based upon research performed in a renovated collaboratory by the National Science Foundation under Grant No. 0963183, which is an award funded under the American Recovery and Reinvestment Act of 2009 (ARRA). The authors wish to thank undergraduate Ryan Wi for his help on the experimental work.

■ REFERENCES

(1) Atsumi, S., Hanai, T., and Liao, J. C. (2008) Non-fermentative pathways for synthesis of branched-chain higher alcohols as biofuels. *Nature 451*, 86−89.

(2) Shen, C. R., and Liao, J. C. (2008) Metabolic engineering of Escherichia coli for 1-butanol and 1-propanol production via the keto-acid pathways. *Metab. Eng. 10*, 312−320.

(3) Lin, P. P., Rabe, K. S., Takasumi, J. L., Kadisch, M., Arnold, F. H., and Liao, J. C. (2014) Isobutanol production at elevated temperatures in thermophilic Geobacillus thermoglucosidasius. *Metab. Eng. 24*, 1−8.

(4) Higashide, W., Li, Y., Yang, Y., and Liao, J. C. (2011) Metabolic Engineering of Clostridium cellulolyticum for Production of Isobutanol from Cellulose. *Appl. Environ. Microbiol. 77*, 2727−2733.

(5) Smith, K. M., Cho, K.-M., and Liao, J. C. (2010) Engineering Corynebacterium glutamicum for isobutanol production. *Appl. Microbiol. Biotechnol. 87*, 1045−1055.

(6) Lin, P. P., Mi, L., Morioka, A. H., Yoshino, K. M., Konishi, S., Xu, S. C., Papanek, B. A., Riley, L. A., Guss, A. M., and Liao, J. C. (2015) Consolidated bioprocessing of cellulose to isobutanol using Clostridium thermocellum. *Metab. Eng. 31*, 44−52.

(7) Li, H., Opgenorth, P. H., Wernick, D. G., Rogers, S., Wu, T.-Y., Higashide, W., Malati, P., Huo, Y.-X., Cho, K. M., and Liao, J. C. (2012) Integrated Electromicrobial Conversion of CO2 to Higher Alcohols. *Science 335*, 1596−1596.

(8) Cann, A. F., and Liao, J. C. (2008) Production of 2-methyl-1-butanol in engineered Escherichia coli. *Appl. Microbiol. Biotechnol. 81*, 89−98.

(9) Connor, M. R., and Liao, J. C. (2008) Engineering of an Escherichia coli Strain for the Production of 3-Methyl-1-Butanol. *Appl. Environ. Microbiol. 74*, 5769−5775.

(10) Raj, K. C., Talarico, L. A., Ingram, L. O., and Maupin-Furlow, J. A. (2002) Cloning and Characterization of the Zymobacter palmae Pyruvate Decarboxylase Gene (pdc) and Comparison to Bacterial Homologues. *Appl. Environ. Microbiol. 68*, 2869−2876.

(11) Thompson, A. H., Studholme, D. J., Green, E. M., and Leak, D. J. (2008) Heterologous expression of pyruvate decarboxylase in Geobacillus thermoglucosidasius. *Biotechnol. Lett. 30*, 1359−1365.

(12) Schwarz, W. H. (2001) The cellulosome and cellulose degradation by anaerobic bacteria. *Appl. Microbiol. Biotechnol. 56*, 634−649.

(13) Liu, J., and Xia, W. (2006) Purification and characterization of a bifunctional enzyme with chitosanase and cellulase activity from commercial cellulase. *Biochem. Eng. J. 30*, 82−87.

(14) Lee, Y.-J., Kim, B.-K., Lee, B.-H., Jo, K.-I., Lee, N.-K., Chung, C.-H., Lee, Y.-C., and Lee, J.-W. (2008) Purification and characterization of cellulase produced by Bacillus amyoliquefaciens DL-3 utilizing rice hull. *Bioresour. Technol. 99*, 378−386.

(15) Ko, C.-H., Tsai, C.-H., Lin, P.-H., Chang, K.-C., Tu, J., Wang, Y.-N., and Yang, C.-Y. (2010) Characterization and pulp refining activity of a Paenibacillus campinasensis cellulase expressed in Escherichia coli. *Bioresour. Technol. 101*, 7882−7888.

(16) Balsan, G., Astolfi, V., Benazzi, T., Meireles, M. A. A., Maugeri, F., Di Luccio, M., Dal Prá, V., Mossi, A. J., Treichel, H., and Mazutti, M. A. (2012) Characterization of a commercial cellulase for hydrolysis of agroindustrial substrates. *Bioprocess Biosyst. Eng. 35*, 1229−1237.

(17) Gocke, D., Nguyen, C. L., Pohl, M., Stillger, T., Walter, L., and Müller, M. (2007) Branched-Chain Keto Acid Decarboxylase fromLactococcus lactis (KdcA), a Valuable Thiamine Diphosphate-Dependent Enzyme for Asymmetric C-C Bond Formation. *Adv. Synth. Catal. 349*, 1425−1435.

(18) Romero, P. A., and Arnold, F. H. (2009) Exploring protein fitness landscapes by directed evolution. *Nat. Rev. Mol. Cell Biol. 10*, 866−876.

(19) Bloom, J. D., Labthavikul, S. T., Otey, C. R., and Arnold, F. H. (2006) Protein stability promotes evolvability. *Proc. Natl. Acad. Sci. U. S. A. 103*, 5869−5874.

(20) Guo, H. H., Choe, J., and Loeb, L. A. (2004) Protein tolerance to random amino acid change. *Proc. Natl. Acad. Sci. U. S. A. 101*, 9205−9210.

(21) Drummond, D. A., Silberg, J. J., Meyer, M. M., Wilke, C. O., and Arnold, F. H. (2005) On the conservative nature of intragenic recombination. *Proc. Natl. Acad. Sci. U. S. A. 102*, 5380−5385.

(22) Aharoni, A., Gaidukov, L., Khersonsky, O., Gould, S. M., Roodveldt, C., and Tawfik, D. S. (2004) The "evolvability" of promiscuous protein functions. *Nat. Genet.*, DOI: 10.1038/ng1482.

(23) Wu, I., and Arnold, F. H. (2013) Engineered thermostable fungal Cel6A and Cel7A cellobiohydrolases hydrolyze cellulose efficiently at elevated temperatures. *Biotechnol. Bioeng. 110*, 1874−1883.

(24) Eiben, C. B., Siegel, J. B., Bale, J. B., Cooper, S., Khatib, F., Shen, B. W., Players, F., Stoddard, B. L., Popovic, Z., and Baker, D. (2012) Increased Diels-Alderase activity through backbone remodeling guided by Foldit players. *Nat. Biotechnol. 30*, 190−192.

(25) Korkegian, A. (2005) Computational Thermostabilization of an Enzyme. *Science 308*, 857−860.

(26) Biasini, M., Bienert, S., Waterhouse, A., Arnold, K., Studer, G., Schmidt, T., Kiefer, F., Cassarino, T. G., Bertoni, M., Bordoli, L., and Schwede, T. (2014) SWISS-MODEL: Modelling protein tertiary and

quaternary structure using evolutionary information. *Nucleic Acids Res. 42*, 252−258.
(27) Berthold, C. L., Gocke, D., Wood, M. D., Leeper, F. J., Pohl, M., and Schneider, G. (2007) Structure of the branched-chain keto acid decarboxylase (KdcA) from *Lactococcus lactis* provides insights into the structural basis for the chemoselective and enantioselective carboligation reaction. *Acta Crystallogr., Sect. D: Biol. Crystallogr. 63*, 1217−1224.
(28) Schrödinger, L. L. C. (2010) *The {PyMOL} Molecular Graphics System*, version 1.3r1, Schrodinger, LLC.
(29) Delaplaza, M., Fernandezdepalencia, P., Pelaez, C., and Requena, T. (2004) Biochemical and molecular characterization of α-ketoisovalerate decarboxylase, an enzyme involved in the formation of aldehydes from amino acids by. *FEMS Microbiol. Lett. 238*, 367−374.
(30) Furey, W., Arjunan, P., Chen, L., Sax, M., Guo, F., and Jordan, F. (1998) Structure-function relationships and flexible tetramer assembly in pyruvate decarboxylase revealed by analysis of crystal structures. *Biochim. Biophys. Acta, Protein Struct. Mol. Enzymol. 1385*, 253−270.
(31) Koga, J., Adachi, T., and Hidaka, H. (1992) Purification and characterization of indolepyruvate decarboxylase. A novel enzyme for indole-3-acetic acid biosynthesis in Enterobacter cloacae. *J. Biol. Chem. 267*, 15823−15828.
(32) Tian, J., Wang, P., Gao, S., Chu, X., Wu, N., and Fan, Y. (2010) Enhanced thermostability of methyl parathion hydrolase from Ochrobactrum sp. M231 by rational engineering of a glycine to proline mutation: Enhanced thermostability of methyl parathion hydrolase. *FEBS J. 277*, 4901−4908.
(33) Guterl, J.-K., Garbe, D., Carsten, J., Steffler, F., Sommer, B., Reiße, S., Philipp, A., Haack, M., Rühmann, B., Koltermann, A., Kettling, U., Brück, T., and Sieber, V. (2012) Cell-Free Metabolic Engineering: Production of Chemicals by Minimized Reaction Cascades. *ChemSusChem 5*, 2165−2172.
(34) Gibson, D. G., Young, L., Chuang, R.-Y., Venter, J. C., Hutchison, C. A., and Smith, H. O. (2009) Enzymatic assembly of DNA molecules up to several hundred kilobases. *Nat. Methods 6*, 343−345.
(35) Atsumi, S., Wu, T.-Y., Eckl, E.-M., Hawkins, S. D., Buelter, T., and Liao, J. C. (2010) Engineering the isobutanol biosynthetic pathway in Escherichia coli by comparison of three aldehyde reductase/alcohol dehydrogenase genes. *Appl. Microbiol. Biotechnol. 85*, 651−657.
(36) Song, Y., DiMaio, F., Wang, R. Y.-R., Kim, D., Miles, C., Brunette, T., Thompson, J., and Baker, D. (2013) High-Resolution Comparative Modeling with RosettaCM. *Structure 21*, 1735−1742.
(37) Gront, D., Kulp, D. W., Vernon, R. M., Strauss, C. E. M., Baker, D., and Uversky, V. N. (2011) Generalized Fragment Picking in Rosetta: Design, Protocols and Applications. *PLoS One 6*, e23294.
(38) Thompson, J., and Baker, D. (2011) Incorporation of evolutionary information into Rosetta comparative modeling. *Proteins: Struct., Funct., Genet. 79*, 2380−2388.

DOI: 10.1021/acssynbio.6b00240
ACS Synth. Biol. 2017, 6, 610−618